ELASTICITY PROPERTIES OF LUNG PARENCHYMA DERIVED FROM EXPERIMENTAL DISTORTION DATA

GEORGE C. LEE *and* ANDREW FRANKUS

From the Department of Civil Engineering, State University of New York at Buffalo, New York 14214

ABSTRACT Distortion data for dog lungs obtained experimentally by Hoppin et al. (1975) are used to arrive at a general mathematical model (strain energy function) which describes finite deformation of lung parenchyma. The strain energy function is correlated with average alveolus model proposed by Frankus and Lee (1974). The latter predicts parenchyma distortion properties from uniformly ventilated pressure-volume data only.

INTRODUCTION

Mead et al. (1970) have shown that nonuniform expansion properties of the lung should be employed to predict lung elasticity behaviors involving inhomogeneities. West and Mathews (1972) have reported analytical results of the distribution of stresses and strains in lungs due to gravitational effect based on more or less estimated elasticity constants of the material. Experimental studies have since been performed by Hoppin et al. (1975) who have derived some nonlinear stress-strain properties for the dog lung. These experimental data are sufficient for the derivation of a single mathematical expression in the form of a strain energy density function W that can fully describe finite deformations of the material (see Lee and Hoppin [1972]). The strain energy function can also be used to obtain the stiffness relationships necessary in finite element methods for analysis of the lung structure. Although the material does not possess a true strain energy function, the derived expression describes the behavior of the material in the lung within the limits of a respiration cycle. It is noted that for saline ventilated lungs, the hysteresis is considered to be negligibly small. Therefore, it is not included in the derivation of the strain energy density function.

In this paper, the forms of the strain-energy function are discussed and the accuracy of the procedures is assessed; the magnitude of the elasticity constants are compared with those reported by Hoppin et al. (1975) and finally, the strain energy function is correlated with the average alveolus model proposed by Frankus and Lee (1974). It may be concluded that the single alveolus model is a simple and reasonably accurate approach in studies of inhomogeneity in lungs.

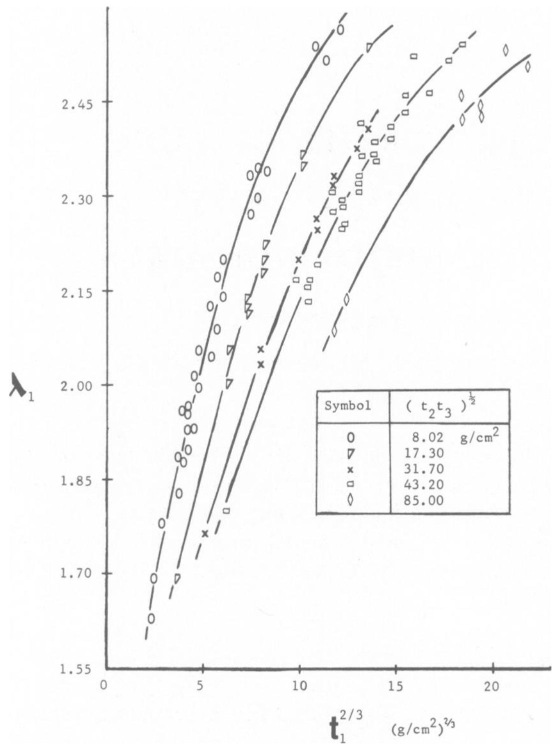

FIGURE 1 Data obtained from experiments on a saline ventilated dog's lung cubes by Hoppin et al. (1975). Common symbols represent constant Lagrangian stresses (t_2 and t_3) while varying t_1 and measuring λ_1. Data are grouped for tests with approximately equal t_2 and t_3 according to explanations given in the Appendix.

UNIAXIAL BEHAVIOR[1]

Data obtained by Hoppin et al. (1975) for a dog lung specimen ventilated in saline are described in Fig. 1. In this figure each fitted curve represents uniaxial stress deformation for different stresses along the other two Cartesian axes which are kept constant for each uniaxial test.[2] Lagrangian stress in the principal stress direction i is identified as t_i and the corresponding nondimensional extension ratio is called λ_i. The adjustments which are made on the experimental data to arrive at the curves in Fig. 2 are explained and justified in the Appendix.

The best fitting curve based on the least squares criterion for the uniaxial test data is found to be of the form

$$\lambda_1 = \mathbf{a}_1 + \mathbf{a}_2 t_1^{2/3} + \mathbf{a}_3 t_1^{4/3}. \tag{1}$$

[1] "Uniaxial behavior" here refers to stretching in one direction while keeping Lagrangian stresses constant in the perpendicular plane. This corresponds with the experimental test procedure of Hoppin et al. (1975).
[2] The 2/3 power used for the stress axis in the graph facilitated the best reasonable polynomial least squares curve fitting.

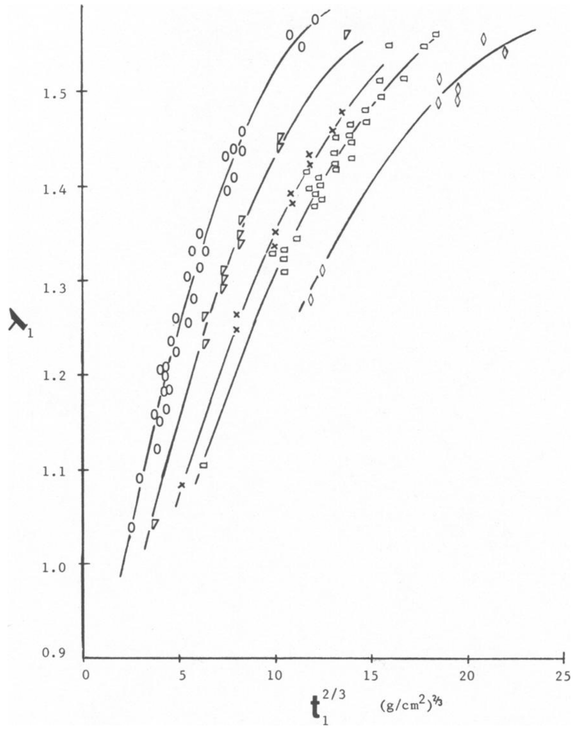

FIGURE 2 Data points of Fig. 1 are replotted after λ_1 has been converted from degassed state to rest state (see Appendix). Symbols are the same as in Fig. 1. The curves in the figure represent Eq. 6 for the same five different constant stresses in the transverse direction (t_2 and t_3) as in Fig. 1.

The coefficients $\mathbf{a}_i$ are functions of the test run parameter t_2t_3. Fig. 3 shows each coefficient plotted against $(t_2t_3)^{1/2}$. After finding the best reasonable model for the curves

$$\mathbf{a}_i = f_i(t_2, t_3) \tag{2}$$

he resulting expression is substituted into Eq. 1. For the saline specimen of Hoppin et al. (1975) it is determined that:

$$\begin{aligned}\lambda_1 = {} & \mathbf{b}_1 + \mathbf{b}_2(t_2t_3)^{1/6} + \mathbf{b}_3(t_2t_3)^{1/3} \\ & + [\mathbf{b}_4 + \mathbf{b}_5(t_2t_3)^{1/6} + \mathbf{b}_6(t_2t_3)^{1/3}]t_1^{2/3} \\ & + [\mathbf{b}_7 + \mathbf{b}_8(t_2t_3)^{1/6} + \mathbf{b}_9(t_2t_3)^{1/3}]t_1^{4/3}.\end{aligned} \tag{3}$$

f the material behaves isotropically (an assumption which can be made for small distortions) then Eq. 3 should be cyclically symmetric with respect to subscripts 1, 2, and 3. In that case Eq. 3 seems to sufficiently describe triaxial stress response of the mate-

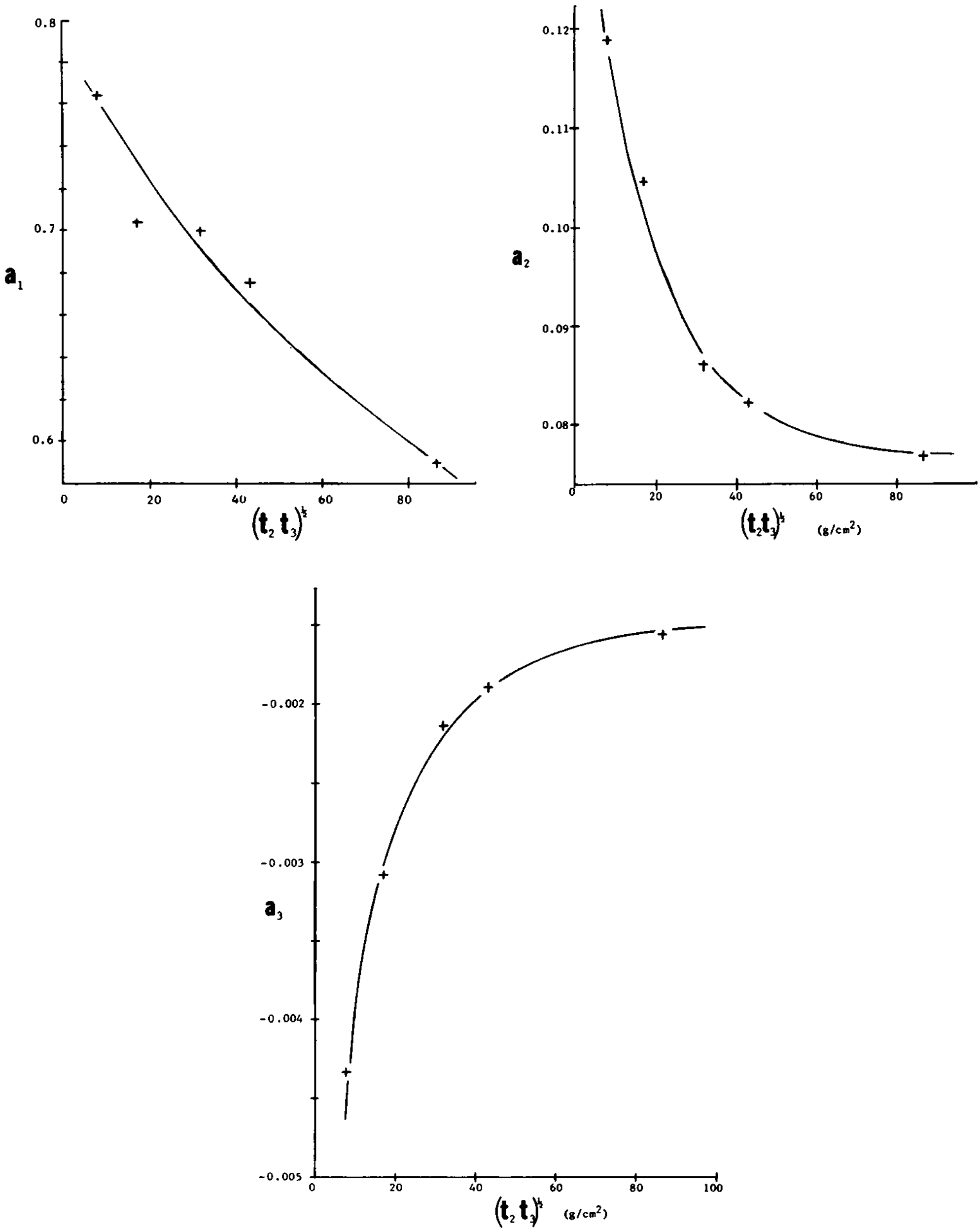

FIGURE 3 Each of the three coefficients of Eq. 1 is plotted vs. the transverse stress parameter $(t_2 t_3)^{1/2}$. Each point on these graphs represents a different one of the five curves in Fig. 2.

rial since it gives λ_i as a function of t_i, or

$$\lambda_i = F_i(t_1\, t_2, t_3). \qquad (4)$$

If Eq. 3 were as sufficiently general as Eq. 4 implies (we know that it applies when $i = 1$), then Eq. 4 could be inverted to yield

$$t_j = \partial W/\partial \lambda_j = G_j(\lambda_1, \lambda_2, \lambda_3). \qquad (5)$$

However, it will be shown in the next section that compressibility characteristics extracted from the specimens are different from those implied in Eq. 4. Nevertheless Eq. 3 is valid as a stress-strain relationship for one principal direction as a function of lateral stress. The inability of Eq. 3 to show corresponding dimensional changes in the perpendicular directions (i.e. compressibility of the material) will be overcome by subsequent inclusion of additional information from experimental data.

The coefficients $\mathbf{b}_i$ in Eq. 3 can obviously be computed in two steps: by first fitting the uniaxial relationship of Fig. 2, and then expressing its coefficients individually as functions of $(t_2t_3)^{1/2}$ (by fitting the curves of Fig. 3). Using Eq. 3 the coefficients for the data of Hoppin et al. (1975) are determined using the least squares criterion for the saline-ventilated specimen:

$$\begin{aligned}\lambda_1 = {} & 1.0 - 0.135\,(t_2t_3)^{1/6} + 0.0105\,(t_2t_3)^{1/3} \\ & + [0.184 - 0.0416\,(t_2t_3)^{1/6} + 0.00383\,(t_2t_3)^{1/3}](t_1)^{2/3} \\ & - [0.00932 - 0.00328\,(t_2t_3)^{1/6} + 0.00034\,(t_2t_3)^{1/3}](t_1)^{4/3}. \end{aligned} \qquad (6)$$

Next, Eq. 6 is evaluated for the five test runs represented by the curves in Fig. 2 where they are superimposed on the original data to validate the results.

EFFECT OF COMPRESSIBILITY

As pointed out earlier, Eq. 6 describes only uniaxial deformation. For large, biaxial distortion, the data for λ_2 and λ_3 reported by Hoppin et al. (1975) have to be incorporated. Since for all of the data, λ_2 and λ_3 are approximately equal, only the effect of compressibility of the material can be extracted. This extraction was accomplished by first plotting λ_1 vs. $\lambda_2\lambda_3$ for each test (i.e. for each constant t_2 and t_3) as given in Fig. 4.

The best fitting relationship found between λ_1, λ_2, and λ_3 is of the form

$$(\lambda_2\lambda_3)^{1/2} = 1 + C_1(\lambda_1^5 - 1) + C_2A + C_3A^2 + C_4A^3, \qquad (7)$$

where $A = (t_2t_3)^{1/8}$

The coefficients C_i are calculated based on least squares fit, and Eq. 7 becomes

$$(\lambda_2\lambda_3)^{1/2} = 1 - 0.092(\lambda_1^5 - 1) - 0.34A + 0.37A^2 - 0.0634A^3. \qquad (8)$$

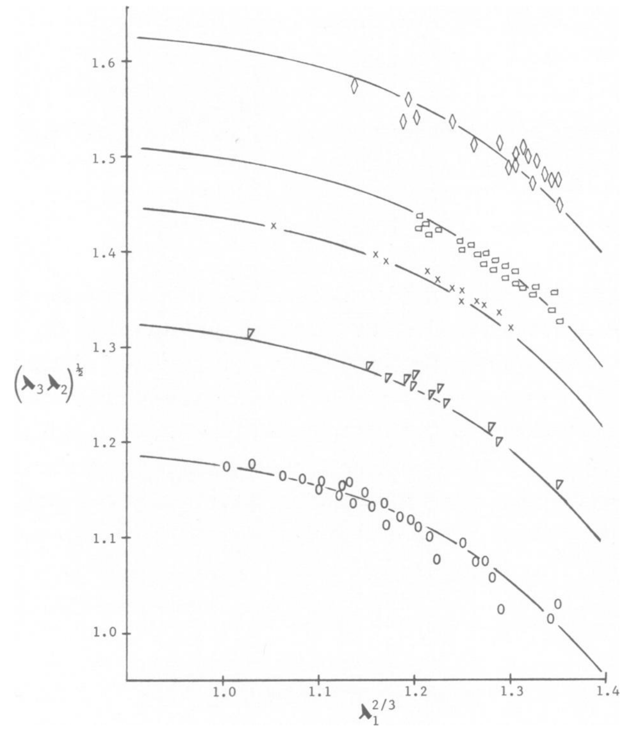

FIGURE 4 Eq. 8 is plotted for the same different constant transverse stresses $(t_2t_3)^{1/2}$. The 2/3 power of the λ_1 coordinate facilitated function form selection and is of no significance to the physical properties of the material. Symbols are the same as in Fig. 1.

The above equations are consistent with the initial condition required when $\lambda_1 = \lambda_2 = \lambda_3 = 1.0$. For this case a root of the remaining three terms gives the result $t_2t_3 = 0$. Eq. 8 is plotted in Fig. 4.

For the uniaxial tension case ($t_2 = t_3 = 0$), Eq. 8 yields the classical Poisson's ratio for infinitesimal uniaxial

$$\nu = [(\lambda_2\lambda_3)^{1/2} - 1]/(\lambda_1 - 1) = 0.092(\lambda_1^4 + \lambda_1^3 + \lambda_1^2 + \lambda_1 + 1) \quad (9)$$

deformation (near $\lambda_1 = 1$) for which Eq. 9 reduces to:

$$\nu = 5(0.092) = 0.46. \quad (10)$$

CONSTITUTIVE RELATIONSHIP

Eqs. 3 and 7 can be solved to yield stresses in terms of strains, or extension ratios, or vice versa. The former can be obtained by first solving Eq. 7 for t_2t_3 and substituting into Eq. 3 to get t_j as a function of the extension ratios (see Eq. 5). This combined form satisfies the initial conditions of zero stress at zero strain. However, a computational advantage results when two equations (3 and 7) are fitted individually to experimental data. The procedure yields Eq. 6 and Eq. 8. If combining in terms of general coefficients, $\mathbf{b}_i$ and C_i, of Eqs. 3 and 7 were possible, the resulting expression would require complex iteration procedures for computing the optimal coefficients. In this study, the fitting procedure in two separate steps requires standard, least-squares regression methods for the determination of the coefficients $\mathbf{b}_i$ and C_j and the lowest positive real root λ of the cubic equation (Eq. 8).

In modeling relatively complex lung elasticity problems the finite element method, as used by West and Mathews (1972), is probably the most suitable procedure. In such a case, a stiffness relationship of the form of Eq. 5 is sufficient. The combined solution of Eqs. 6 and 8 would provide the information when using the incremental finite element methods. In problems of simple geometry for which solutions can be obtained by theoretical elasticity methods, the strain energy density function W or a suitable stress-strain relationship itself is needed. The derivation of this function for the lung parenchyma considered in this study is discussed in the following section.

STRAIN-ENERGY FUNCTION

Since a constitutive relationship is now available in the form of a continuous function, a strain energy density function is next obtained by first assuming a function form and then fitting its parameters into data points generated from the constitutive function.

The advantages of this approach over direct utilization of experimental data, are as follows:

(*1*) Experimental inconsistencies are removed at each step in this procedure, thus smoothing of data is achieved. This allows the use of more stringent quantitative criteria in the subsequent fitting process.

(*2*) A greater quantity of data points can be generated, especially in regions such as the stress-free state where constraints, based on physical requirements for material behavior, should be imposed and in regions where the quantity of experimental data is insufficient.

The strain energy of an elastic continuum is generally expressed as a function of strain:

$$W = W(e_{ij}). \tag{11}$$

For a nonlinear material W can be expressed as an infinite power series in e_{ij}, or it can be approximated by a complete polynomial of order n with a finite number of terms. Normally, it is necessary to express the strain energy function in terms of parameters which are invariant with respect to coordinate transformations (I_1, I_2, I_3). Then, the extension ratio λ_i can be substituted for strain in Eq. 11 from the relationship:

$$e_{ii} = \tfrac{1}{2}(\lambda_1^2 - 1). \tag{12}$$

Based on Eq. 12 it is reasonable to assume that W can be approximated by a polynomial in even powers of λ_i,

$$W = \sum_k C_{ijk} \lambda_i^l \lambda_j^{k-l}, \tag{13}$$

where $i,j = 1,2,3$; $k = 2,4,6,\ldots n$; and $l = 0,2,4,\ldots k$.

There are a large number of other possibilities in choosing the functional form in terms of e_{ij}, λ_i, I_i, including an exponential function proposed by Fung (1974). After a number of trials with the available experimental data, Eq. 13 gave the best results. Since the material is initially isotropic, Eq. 13 must be cyclically symmetric in i and j. Therefore, C_{ijk} will vary only with varying k and l. This means that similar terms can be lumped to reduce the number of arbitrary coefficients. Using $n = 8$ in Eq. 13, the complete expression becomes,

$$\begin{aligned} W = {} & \sum_{i=1}^{4} a_i(\lambda_1^{2i} + \lambda_2^{2i} + \lambda_3^{2i}) + \sum_{i=1}^{2} b_i(\lambda_1^{2i}\lambda_2^{2i} + \lambda_2^{2i}\lambda_3^{2i} + \lambda_1^{2i}\lambda_3^{2i}) \\ & + c_1(\lambda_1^2\lambda_2^2\lambda_3^2) + \sum_{i=2}^{3} c_i(\lambda_1^{2i}\lambda_2^2 + \lambda_2^{2i}\lambda_3^2 + \lambda_3^{2i}\lambda_1^2 \\ & + \lambda_1^2\lambda_2^{2i} + \lambda_2^2\lambda_3^{2i} + \lambda_3^2\lambda_1^{2i}). \end{aligned} \tag{14}$$

In terms of the familiar strain invariants I_i,

$$\begin{aligned} I_1 &= \lambda_1^2 + \lambda_2^2 + \lambda_3^2 \\ I_2 &= \lambda_1^2\lambda_2^2 + \lambda_2^2\lambda_3^2 + \lambda_1^2\lambda_3^2 \\ I_3 &= \lambda_1^2\lambda_2^2\lambda_3^2, \end{aligned} \tag{15}$$

the strain energy function may be expressed as:

$$\begin{aligned} W = {} & a_1I_1 + a_2(I_1^2 - 2I_2) + a_3(I_1^3 - 3I_1I_2 + 3I_3) + a_4(I_1^4 - 4I_1^2I_2 \\ & + 2I_2^2 + 4I_1I_3) + b_1I_2 + b_2(I_2^2 - 2I_1I_3) + c_1I_3 + c_2(I_1I_2 - 3I_3) \\ & + c_3(I_1^2I_2 - 2I_2^2 - I_1I_3). \end{aligned} \tag{16}$$

Eq. 14 includes terms with even powers of λ_i up to the power of 8 (i.e., 2,4,6,8). The criterion for including these terms is based on the relatively small value of the sum-of-squares of the errors (see Table I).[3]

The experimentally measured stresses, shown in Table II, are compared with stresses computed from the strain energy function of Eq. 16. The corresponding coefficients in Eq. 14 for this case have the following values (with units of grams per square

[3] The error is defined as the difference between t_i in row A and t_i in row B of Table II.

TABLE I

RELATIVE ACCURACY FOR INCREASING NUMBER OF TERMS IN STRAIN ENERGY FUNCTION

No. of terms	Coefficients of Eq. 14	Max. power of λ_i	$\Sigma(\text{error})^2$
1	a_1	2	7,321
3	a_1, a_2, b_1	4	470
6	a_1, a_2, a_3 b_1, c_1, c_2	6	153
9	a_1, a_2, a_3, a_4 b_1, b_2, c_1, c_2, c_3	8	105

centimeters):

$$\begin{aligned} a_1 &= -21.06 & b_1 &= 2.673 & c_1 &= 1.324 \\ a_2 &= 19.76 & b_2 &= -0.350 & c_2 &= -1.94 \\ a_3 &= -7.88 & & & c_3 &= 0.943 \\ a_4 &= 1.062 & & & & \end{aligned} \tag{17}$$

In this case Eq. 14 does not satisfy the initial condition $\partial^2 W/\partial \lambda_i^2 = 0$.[4] However, this will have only relatively small influence near the stress-free condition and is of less significance from the physiological point of view.

The data points selected for comparison in Table II are: all data whose relative order of magnitude of stress (experimentally measured) is consistent, or almost consistent, with corresponding extension ratios and all readings which are repeated at least once. The averages of those repeated readings are also given in Table II, row A. Lagrangian stresses of row B are simply the first derivatives of W of Eq. 14 with respect to the corresponding λ_i.

THE AVERAGE ALVEOLUS MODEL

All the equal triaxial experimental data reported by Hoppin et al. (1975) are plotted in Fig. 5. This curve was used as the only input for the single alveolus model proposed by Frankus and Lee (1974) for the purpose of computing distortion characteristics of the lung parenchyma. A comparison of stresses based on the average alveolus concept and on Eq. 14 are given in Table II together with the experimental data. This "average alveolus" model, also proposed independently by Fung (1974), and by Lee and Soong (1973), seems to be a reasonable and convenient approach for analyzing distortion properties of the lung parenchyma because it requires only the pressure-volume (equal triaxial) relationship of the lung.

[4] Experiments on lung material show that resistance against initial, infinitesimal displacements approaches zero as deformation approaches zero, hence: $\partial^2 W/\partial \lambda_1^2 = 0$; at $\lambda_1 = 1.0$.

TABLE II

COMPARISON OF RESULTS WITH EXPERIMENTAL DATA

λ_1	λ_2	λ_3	*	t_1	t_2	t_3
1.198	1.148	1.153	A	8.7	7.4	8.0
			B	8.6	7.0	7.2
			C	9.4	7.5	7.7
1.213	1.121	1.178	A	9.7	7.4	8.7
			B	9.3	6.3	8.1
			C	10.1	6.8	8.8
1.227	1.142	1.160	A	10.6	7.4	8.0
			B	10.0	7.1	7.7
			C	11.0	7.6	8.3
1.240	1.133	1.135	A	10.6	7.4	8.0
			B	10.3	6.7	6.7
			C	11.4	7.1	7.3
1.248	1.275	1.294	A	16.0	16.6	18.0
			B	15.8	17.0	18.1
			C	16.4	18.3	19.5
1.256	1.406	1.398	A	22.4	30.5	33.0
			B	22.8	35.6	34.7
			C	21.7	37.8	35.5
1.303	1.266	1.286	A	19.6	16.6	18.0
			B	19.5	17.3	18.5
			C	21.0	18.3	19.9
1.309	1.093	1.135	A	13.9	7.4	8.7
			B	13.8	6.0	7.2
			C	15.6	6.3	7.7
1.315	1.112	1.120	A	15.1	7.4	8.0
			B	14.3	6.7	6.9
			C	16.3	6.9	7.3
1.352	1.252	1.263	A	23.3	16.6	18.0
			B	23.4	17.0	17.6
			C	25.6	17.5	18.5
1.401	1.397	1.418	A	43.0	39.7	46.9
			B	41.8	41.3	44.0
			C	42.2	41.8	44.7
1.427	1.048	1.093	A	22.2	7.4	8.7
			B	22.3	6.3	7.5
			C	25.9	5.8	6.8
1.441	1.391	1.405	A	51.3	39.7	46.9
			B	48.7	41.7	43.5
			C	49.6	41.9	43.9
1.449	1.042	1.047	A	24.2	7.4	8.0
			B	23.5	6.2	6.3
			C	27.9	5.5	5.3
1.449	1.215	1.224	A	32.4	16.6	18.0
			B	34.2	16.6	17.1
			C	37.4	15.9	16.7
1.452	1.385	1.402	A	51.3	39.7	46.9
			B	50.5	41.1	43.2
			C	51.5	40.8	43.6

*A, experimental data; B, from strain energy function based on test data; C, based on average alveolus concept.

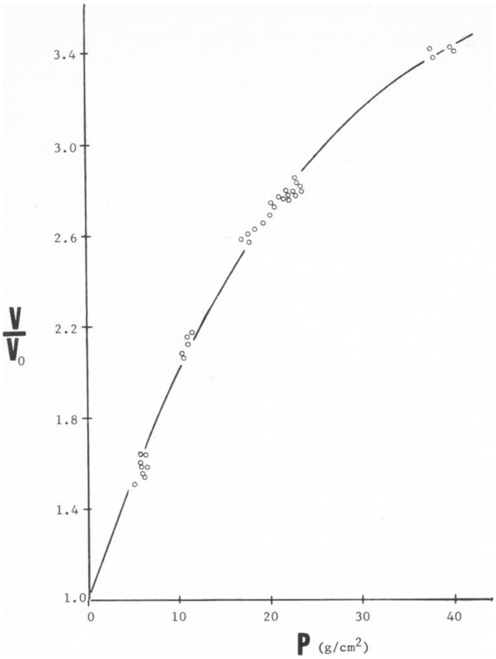

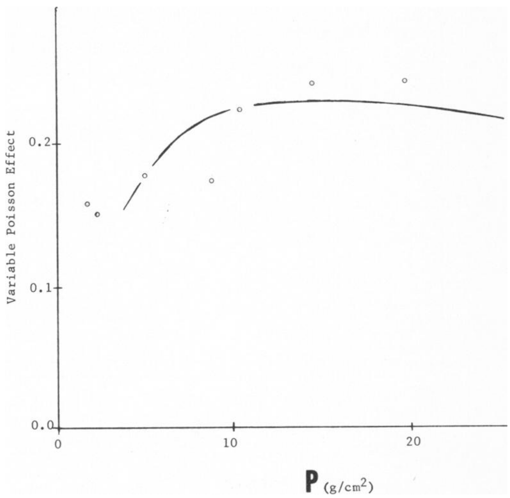

FIGURE 5

FIGURE 6

FIGURE 5 The pressure-volume relationship (normalized with respect to initial volume) for the saline-ventilated dog lung specimen extracted from the data of Hoppin et al. (1975). This curve is used as the only input for generating triaxial test data via the single alveolus model of Frankus and Lee (1974).

FIGURE 6 The strain energy function of Eq. 16 with coefficients of Eq. 17 is used to determine the variable Poisson effect computed as $d\lambda_{axial}/d\lambda_{lat}$ at varying values of initial uniform expansion in terms of uniform true stress. The result is the continuous curve. The points plotted in the figure are experimental results obtained by Hoppin et al. (1975) for saline ventilated dog lungs. The curve cannot be extrapolated to zero pressure since the function W of Eq. 16 does not represent the region near zero stress.

COMPARISON OF SPECIFIC MATERIAL PROPERTIES

Although Eq. 10 reflects the constant Poisson's ratio of the material for small uniaxial deformations only, a "variable Poisson effect" is of interest in lung elasticity studies. This is also defined as "the ratio of change of strain in the lateral direction (λ_2, λ_3) to a change of strain in the longitudinal direction (λ_1) for constant stress (t_2, t_3) in the lateral direction." This property is plotted as a curve in Fig. 6 which also shows for comparison the equivalent data points for the material from Hoppin et al. (1975).

Young's modulus (tangent modulus), also derived from Eq. 14 for equal expansion, is superimposed on data from Hoppin et al. (1975) in Fig. 7. The last two figures are plotted versus uniform initial pressure. The bulk modulus calculated from Eq. 14, as the change in volume caused by a small increment of uniaxial stress superimposed on

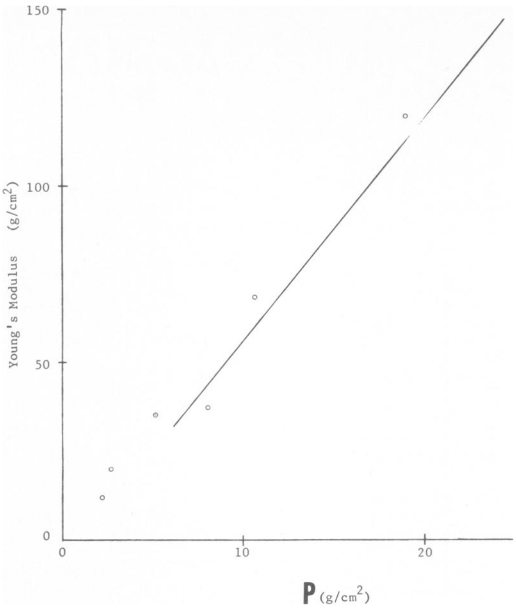

FIGURE 7

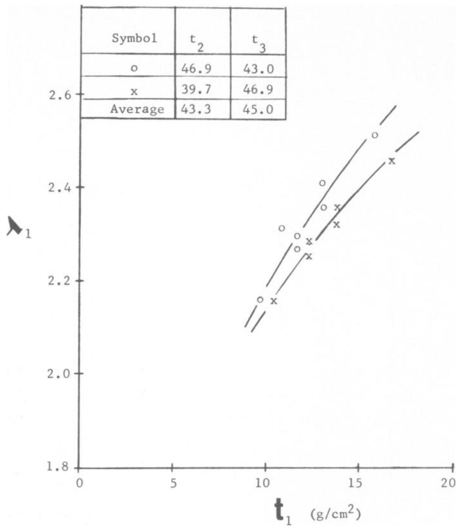

FIGURE 8

FIGURE 7 Derived from the strain energy function (as in Fig. 6) the varying Young's modulus is represented by the straight line. The points are for saline-ventilated dog lungs as reported by Hoppin et al. (1975). As in Fig. 6, the results are for small distortion superimposed on uniform expansions at indicated uniform expansion pressure.

FIGURE 8 Two individual test runs (constant t_2, t_3, varying λ_1 and t_1) are shown before they were averaged to represent a single average test because of experimental inconsistencies evident from this graph and explained in the text.

uniform expansion, was about 40% lower than that shown by Hoppin et al. (1975). No explanation can be given for this discrepancy.

SUMMARY

The mathematical expressions derived in this paper are based on experimental data for distortional characteristics of dog lungs ventilated in saline. Physical constraints for the material not sufficiently reflected by the data are imposed on the constitutive relationships. Next, analytical data are computed from the derived equations after the experimental data have been smoothed, interpolated, and strengthened at the extreme points of the experimental range of distortion.

The analytically-generated data are validated by comparing them with the original test data. They are also compared against results obtained from the single alveolus model proposed by Frankus and Lee (1974) within the limits of distortion (approx. 50%) of the experimental data.

These calculated data are then utilized to determine the strain-energy function W. The general form of W is expected to be able to describe behavior of other mammalian

lungs ventilated in saline when its coefficients are statistically optimized for the specific lung parenchyma in question.

W is validated by extracting stresses and specific material properties analytically from W and comparing them against the test data reported by Hoppin et al. (1975).

The authors extend their appreciation to Dr. Michael L. Morrell for his valuable suggestions and comments.

This research is supported by a National Heart and Lung Institute grant (no. 1RO1HL1449501A1).

Received for publication 7 November 1974.

REFERENCES

FRANKUS, A., and G. C. LEE. 1974. A theory for distortion studies of lung parenchyma based on alveolar membrane properties. *J. Biomech.* **7**:101.

FUNG, Y. C. 1974. A theory of elasticity of the lung. *J. Appl. Mech.* **41**:8.

GREEN, A. E., and J. E. ADKINS. 1970. Large Elastic Deformations. Clarendon Press, Oxford. 2nd edition. 8–10.

HOPPIN, F. G., G. C. LEE, and S. V. DAWSON. 1975. Properties of lung parenchyma in distortion. *J. Appl. Physiol.* In press.

LEE, G. C., and F. G. HOPPIN. 1972. Lung elasticity. *In* Biomechanics—Its Foundations and Objectives. Prentice-Hall, Inc., Englewood Cliffs, N.J. 317–335.

LEE, G. C., and T. T. SOONG. 1973. Elastic recoil characteristics of lungs based on a model of averaged alveolus. Proceedings of the 10th Annual Meeting of the Society of Engineering Science, Nov. 1973.

MEAD, J., T. TAKASHIMA, and D. LEITH. 1970. Stress distribution in lungs: a model of plumonary elasticity. *J. Appl. Physiol.* **28**:596.

WEST, J. G., and F. L. MATHEWS. 1972. Stresses, strains and surface pressures in the lung caused by its weight. *J. Appl. Physiol.* **32**:332.

APPENDIX

Adjustment of Experimental Data

The data obtained by Hoppin et al. (1975) is found to contain small inconsistencies which required compensation because of the sensitivity of the mathematical methods used in this study. The most severe example is shown in Fig. 8 where two uniaxial test runs are compared for the same saline ventilated specimen. Higher constant stress in the 2- and 3-direction shows a higher extension ratio in direction 1 which implies a negative Poisson's ratio and is also inconsistent with the general trend exhibited in Figs. 1 and 2. As a remedy, results from the two tests are lumped together and used as a single test with equivalent lateral stresses (t_2 and t_3) which are the average of the two. Additional adjustment is required to yield a unit reference volume ($\lambda_1\lambda_2\lambda_3 = 1.0$) at zero stress. This requirement does not imply a lack of precision in the data, which were referenced to a gas free state (Hoppin et al. [1975]). In order to obtain a strain energy expression whose variables are consistent with their definitions, all extension ratios are divided by a constant value of 1.63. This value is used to arrive at an extension ratio of 1.0 at zero stress and is consistent with the basis for measurement during the experiment by Hoppin et al. (1975).